Adaptive optical multi-aperture receive antenna for coherent intersatellite communications

Klaus H. Kudielka, Wolfgang M. Neubert, Arpad L. Scholtz, Walter R. Leeb

Institut für Nachrichtentechnik und Hochfrequenztechnik, Technische Universität Wien
Gußhausstraße 25/389, A-1040 Wien, Austria

ABSTRACT

The concept of an adaptive receive telescope array (RTA) for coherent optical space communications is presented. The RTA consists of $N=2^K$, e.g. 16, subtelescopes, N polarization-maintaining single-mode fibers, N optical phase actuators, a binary tree of N-1 symmetrical polarization-maintaining directional couplers, N-1 optical power sensors, and a digital control unit. The output interface, a polarization-maintaining single-mode fiber, can be efficiently coupled to a subsequent coherent receiver. Within a subtelescope's field-of-view, the control unit adapts the subtelescope phases (pistons) to the direction of the incident wavefront, thus maximizing the strength of the optical output field. The RTA is transparent, i.e. it operates independently of the modulation format employed. The feasibility of the RTA concept was demonstrated in a laboratory experiment. The implemented four-aperture antenna operates at a wavelength of 1064nm. At an optical power level of 1nW per subaperture, the experimental system combines the optical input signals with an efficiency greater than 99%. A step-shaped change of input wavefront direction is automatically compensated within 1ms.

1. INTRODUCTION

Phased telescope arrays offer a wide range of applications. They can be used to correct atmospheric turbulence,[1,2] to obtain high angular resolution images,[3] to implement wide field-of-view imaging systems,[4] or to coherently receive or transmit optical radiation.[5,6,7,8] For coherent optical space communications, multi-aperture receive antennas provide non-mechanical, self-adaptive fine steering of the main lobe direction, thus compensating satellite attitude jitter. Additional benefits of a receive telescope array (RTA) over a single, large telescope are modularity, ease of fabrication, and implicit redundancy.

Several conditions have to be met in a coherently operating telescope array. First, the optical lengths of the individual subtelescope paths are to be actively controlled with an accuracy better than a tenth of a wavelength. Second, the axes of the individual subtelescopes should be aligned in parallel. In an operational system the required subtelescope tilt tolerance[9] may be achieved by intermittent readjustment. The third prerequisite for efficient coherent superposition of subaperture radiation is a close coincidence of the state of polarization. This requirement can be fulfilled by the use of polarization-maintaining components throughout the optical setup.

For optimum RTA efficiency, the subtelescope fields have to be superimposed coaxially.[10] This can be achieved either in the optical regime (by beam splitters or fiber directional couplers) or in the electrical intermediate frequency domain (by RF directional couplers). The electrical approach, already demonstrated by Mercer,[6] is very complex. High-data-rate receiver electronics are required for every single subtelescope path. We propose a system based on optical subfield superposition. This results in a much simpler, transparent array antenna system which operates independently of the subsequent optical receiver.

2. PISTON CONTROL CONCEPT

Optical path length control and subfield superposition define the structure of a phased RTA. In Sect. 2.1 we develop an elementary RTA which phases and superimposes two optical subfields, combining both fields to a single output. In Sect. 2.2 we generalize the piston control concept to $N=2^K$ subtelescopes by cascading elementary beam combiners.

2.1. Elementary beam combiner

Figure 1 shows an elementary beam combiner. A 50:50 polarization-maintaining single-mode directional coupler is fed by two subtelescope fields of equal powers $P_1=P_2=P$ and of phases φ_1 and φ_2. The phase difference $\varphi_1-\varphi_2$ is adjusted by a piston actuator. An optical power sensor detects the output power at port B,

$$P_B = P\left(1-\cos\left(\varphi_1-\varphi_2\right)\right) \quad . \tag{1}$$

The desired phase difference is $\varphi_1-\varphi_2=0$, implying $P_B=0$ and, at output port A, $P_A=2P$. Sinusoidally dithering around the operating point (amplitude $\Delta\varphi_d$, frequency f_d) causes the power sensor to detect a signal at f_d and its multiples. It is sufficient to synchronously demodulate the signal at f_d into the baseband. The resulting phase detector voltage V_{PD} is

$$V_{PD} = G\,S\,P\Delta\varphi_d\,\sin\left(\varphi_1-\varphi_2\right) \quad , \tag{2}$$

where G denotes the gain of the demodulator and S is the sensitivity of the optical power sensor. In combination with a loop filter and an integrator V_{PD} is used to close an optical phase-locked loop (OPLL). The dither frequency f_d must be higher than the bandwidth of the phase-locked loop, B_L, and the dither amplitude must be very small compared to 2π. Typical values are B_L=2kHz, f_d=10kHz, and $\Delta\varphi_d$=0.1rad. The OPLL locks at $\varphi_1-\varphi_2=0$ and directs the total optical input power 2P to output port A.

2.2. Cascading elementary beam combiners

If more than N=2 subtelescope signals have to be combined we can cascade the simple structure shown in Fig. 1 to form a binary tree. The expanded RTA would consist of $N=2^K$ subtelescopes, N-1 directional couplers, N-1 piston actuators, N-1 optical power sensors, N-1 piston control loops, and a single output waveguide. Now it is expedient to separate the process of phase shifting and that of subfield superposition. The resulting RTA structure for N=8 subtelescopes is depicted in Fig. 2. The piston control unit drives the N piston actuators with the aim to minimize the N-1 error signals, thus automatically maximizing the optical output power.

For (N-1)-fold minimum finding the piston control unit could employ multiple dither frequencies.[11] This approach is very complex and requires high-bandwidth piston acuators. For the present RTA structure we found a control algorithm which uses only a single dither frequency. This algorithm is outlined in the following.

The normalized optical fields feeding the binary tree of directional couplers are

$$a_k = \exp\left[\,j\left(\varphi_k + d_k\Delta\varphi_d\,\sin\omega_d t\right)\right] \quad , \quad k=1..N \quad , \tag{3}$$

where φ_k denotes the piston of subtelescope k shifted by phase actuator k and d_k is what we call dither factor ($d_k \in \{-1,0,+1\}$). The d_k have to be chosen such that, after synchronously demodulating each optical power sensor output at the dither frequency $\omega_d=2\pi f_d$ the optical phase difference at the pertinent directional coupler can be measured (see Fig. 2). Figure 3 shows any of the optical power sensors within the binary tree, the pertinent directional coupler, and two subtrees feeding the coupler with fields

$$\alpha = \frac{1}{\sqrt{M}}\sum_{k=L}^{L+M-1} a_k \quad \text{and} \quad \beta = \frac{1}{\sqrt{M}}\sum_{k=L+M}^{L+2M-1} a_k \quad . \tag{4}$$

The optical power sensor detects the normalized optical power

$$p = \left|\frac{\alpha-\beta}{\sqrt{2}}\right|^2 = \frac{1}{2M}\left|\sum_{k=L}^{L+M-1} a_k - \sum_{k=L+M}^{L+2M-1} a_k\right|^2 \quad , \tag{5}$$

which can also be expressed as

$$p = 1+\frac{1}{M}\left[\sum_{k=L}^{(L+M-2)}\sum_{l=k+1}^{(L+M-1)} p_{kl} + \sum_{k=L+M}^{(L+2M-2)}\sum_{l=k+1}^{(L+2M-1)} p_{kl} - \sum_{k=L}^{(L+M-1)}\sum_{l=L+M}^{(L+2M-1)} p_{kl}\right] \tag{6}$$

with

$$p_{kl} = \mathrm{Re}\left\{a_k a_l^*\right\} = \cos\left[\left(\varphi_k-\varphi_l\right)+\left(d_k-d_l\right)\Delta\varphi_d \sin\omega_d t\right] \quad , \tag{7}$$

where the asterisk denotes the complex conjugate. Synchronously demodulating p at ω_d yields (compare Fig. 3)

$$\tilde{p} = \frac{1}{M}\left[\sum_{k=L}^{(L+M-2)}\sum_{l=k+1}^{(L+M-1)} \tilde{p}_{kl} + \sum_{k=L+M}^{(L+2M-2)}\sum_{l=k+1}^{(L+2M-1)} \tilde{p}_{kl} - \sum_{k=L}^{(L+M-1)}\sum_{l=L+M}^{(L+2M-1)} \tilde{p}_{kl}\right] \tag{8}$$

with

$$\tilde{p}_{kl} = -\Delta\varphi_d\left(d_k-d_l\right)\sin\left(\varphi_k-\varphi_l\right) \quad , \tag{9}$$

where we assumed $\Delta\varphi_d << \pi$.

Equations (8) and (9) allow to investigate both operating modes of the piston control loop, i.e. tracking and acquisition. We first concentrate on tracking, thus assuming small phase errors (φ_k-φ_l). Hence we can simplify Equ. (9) to

$$\tilde{p}_{kl} = -\Delta\varphi_d\left(d_k-d_l\right)\left(\varphi_k-\varphi_l\right) \quad . \tag{10}$$

Inserting Equ. (10) into Equ. (8) yields

$$\tilde{p} = \frac{D\Delta\varphi_d}{M}\left(\sum_{k=L}^{L+M-1}\varphi_k - \sum_{k=L+M}^{L+2M-1}\varphi_k\right) \tag{11}$$

where

$$D = \sum_{k=L}^{L+M-1} d_k - \sum_{k=L+M}^{L+2M-1} d_k \quad . \tag{12}$$

Equation (11) reveals that, for small phase errors, each piston control loop detects the difference between the arithmetic mean of pistons L through L+M-1 and the arithmetic mean of pistons L+M through L+2M-1 (see Fig. 3). After filtering and integrating the piston error signal (compare Fig. 1), the control signal is applied to piston actuators L through L+M-1, and the negative control signal is applied to actuators L+M through L+2M-1. By this measure the control loops do not influence each other. Equation (12) prescribes the dither factors, d_k: The factor D must not become zero for any of the N-1 control loops. Figure 4 illustrates how to find d_k. Each node of the binary tree is assigned a value $d \in \{-1,0,+1\}$. Each node value has to be the sum of the values of both subnodes. The circled values at the bottom level are the dither factors. The tree

and the node values are generated from top to bottom. A node with d=0 yields subnodes with d=1 and d=-1; one with d=1 yields subnode values d=1 and d=0; one with d=-1 yields d=0 and d=-1, thus fulfilling Equ. (12).

To investigate the acquisition process within any piston control loop, we can proceed from the fact that all control loops within both subtrees are already locked (see Fig. 3), i.e.

$$\varphi_\alpha = \varphi_L = \ldots = \varphi_{L+M-1} \quad \text{and} \quad \varphi_\beta = \varphi_{L+M} = \ldots = \varphi_{L+2M-1} \quad . \tag{13}$$

Inserting Equs. (9) and (13) into Equ. (8) yields

$$\tilde{p} = D\Delta\varphi_d \sin\left(\varphi_\alpha - \varphi_\beta\right) \quad . \tag{14}$$

Again, the dither factors d_k must be chosen to yield $D \neq 0$. Because of the sinusoidal phase detector characteristic, every piston control loop within the binary tree automatically acquires the operating point $\varphi_\alpha = \varphi_\beta$ and thus enters the tracking mode.

3. RECEIVE ANTENNA DEMONSTRATOR

The feasibility of phased telescope arrays operating in receive mode and especially the function of the piston control concept discussed in Sect. 2 were verified by a proof-of-principle experiment.

3.1. Block diagram

Figure 5 shows the block diagram of the experimental four-aperture receive antenna. The system operates at a wavelength of 1064nm. Four closely spaced lenses (3mm diameter each) couple the homogeneous plane input wave into four polarization-maintaining single-mode fibers. Piezo-electric fiber stretchers set the relative pistons of the optical subwaves propagating to the tree of fiber directional couplers. If correct phase relationships prevail, the incident optical radiation is coherently collected and directed to the antenna output fiber. By driving the piezo-electric fiber stretchers, the piston control unit shown in Fig. 5 automatically adapts the pistons of the subaperture fields so that the optical powers in fibers B, C, and D are minimized. Hence, within the field-of-view of a single subaperture, the antennna output power available for the subsequent receiver is automatically maximized, independent of the direction of the incident wavefront.

3.2. Control electronics

For the four-aperture RTA we use a single dither frequency of f_d=10kHz. The dither amplitude is $\Delta\varphi_d$=0.1rad, and the dither factors are d_1=1, d_2=0, d_3=0, and d_4=-1. Figure 6 depicts the resulting block diagram of the piston control unit. To decouple the three OPLLs, the integrator outputs are linearly combined according to Sect. 2.2. The resulting four control signals are applied to the piston actuators shown in Fig. 5.

Two interchangeable versions of the piston control unit were implemented. The analog control unit consists entirely of standard electronic circuits. The digital piston control unit is based on the ADSP-2101 digital signal processor. Since both units use the same control algorithm, their performance is very similar.

3.3. Measurement results

The experimental RTA was designed for an on-axis optical output power of 4nW. At this low power level we measured an excellent phasing efficiency[8] of 99.7%, i.e. only 0.3% of the available optical power are lost due to dithering and optical power sensor noise. The probability for a reduction of the antenna output power by more than 1% remains below 10^{-6}. After a step-like change of the input wave direction, the system adapts the optical subfield phases within 1ms. The measured antenna pattern, i.e. output power vs. angle of incidence, shows good correspondence with theory. The full-width, half-maximum acceptance angle of the experimental RTA was determined to be 0.44mrad, slightly broader than the field-of-view of a single subtelescope (0.42mrad).

4. PROPOSED 16-APERTURE RECEIVE ANTENNA

Based on the piston control concept discussed in Sect. 2 and on the experience gained with the laboratory demonstrator, a preferred concept of an operational 16-aperture receive antenna has been devised.

4.1. Block diagram

Figure 7 shows the block diagram of the proposed RTA. The telescope array unit collects the incident optical radiation and couples it into 16 polarization-maintaining single-mode fibers. The fibers feed the beam combiner module where each optical subwave is first shifted in phase by a piston actuator. Then the subbeams are superimposed by a binary tree of 15 directional couplers. Both input ports of each coupler carry substantially equal optical powers. The signal output port nominally carries the total optical input power. The control output port of each coupler, where the optical power has to be minimized, feeds an optical power sensor. The signal output port of the last directional coupler constitutes the antenna output. The piston control unit drives the 16 piston actuators so that the 15 piston error signals are minimized, thus directing the total available optical power to the subsequent receiver.

Subtelescope tilts may have to be adjusted now and then. To this end, the leftmost 8 piston control loops are inverted one by one, causing the corresponding optical power sensor to be fed by the coherent sum of two subtelescope fields. The tilt adjustment unit shown in Fig. 7 successively adjusts the tilts of the two pertinent subtelescopes for maximum optical power. Finally, the control loop is switched back to normal polarity. Because just one of the 8 tilt control processes is active at a time, only two subtelescopes are out of operation and the receiver sees only slightly reduced optical power. Hence communication will not necessarily be interrupted during tilt readjustment. A coarse pointing control signal may be obtained by conically scanning the telescope array unit and measuring the antenna output power. Calculated orbit data may support this process.

4.2. Telescope array module

The suggested structure of the telescope array module is shown in Fig. 8. The 16 subtelescopes, arranged on a Cartesian grid, collect the incoming, circularly polarized radiation and couple it into the polarization-maintaining single-mode fibers. The fiber ends are equipped with quarter-wave plates which convert the circular state of polarization of each subwave into the linear state of polarization required by the polarization-maintaining fibers. Each quarter-wave plate is anti-reflection-coated on the input side to avoid multiple reflections within the fiber-optic setup. Piezo-electric translators allow two-dimensional lateral movement of each fiber end in order to minimize the relative subtelescope tilts. A coarse mechanism points the telescope array module towards the optical transmitter with an accuracy better than the diffraction-limited divergence of a single subtelescope.

5. CONCLUSION

Phased telescope arrays allow the realization of large collecting apertures without the need of fabricating large-diameter optics. At the same time, the pointing accuracy requirement is reduced to that of a small subtelescope. The implementation of active piston control poses no serious problems for an operational system, even in case of a large number of subapertures and limited piston actuator bandwidth. The beam combining and piston control concept features low complexity and allows light and compact setups. Integrated optics techology can eventually be used profitably for implementing piston actuators, directional couplers, and optical power sensors. These considerable advantages encourage the use of telescope arrays in coherent optical space communication links.

6. ACKNOWLEDGMENTS

The contents of this paper evolved from a research project supported by the European Space Agency (ESA). We wish to thank Alex Popescu and Bernhard Furch for monitoring and supporting this work. We also thank all the students who contributed to the successful realization and the testing of the experimental setup.

7. REFERENCES

1. J. E. Pearson, "Atmospheric Turbulence Compensation using Coherent Optical Adaptive Techniques", Appl. Opt., Vol. 15, No. 3, pp.622-631, March 1976.

2. C. L. Hayes et al., "Experimental Test of an Infrared Phase Conjugation Adaptive Array", J. Opt. Soc. Am., Vol. 67, No. 3, March 1977.

3. P. Wizinowich et al., "Adaptive Optics for Array Telescopes using Piston-and-Tilt Wavefront Sensing", Appl. Opt., Vol. 31, No. 28, pp. 6036-6046, October 1992.

4. C. R. DeHainaut et al., "Wide Field of View Phased Array Telescope", Proc. SPIE, Vol. 1236, pp. 456-462, 1990.

5. J. S. Fender et al., "Demonstration of an Optically Phased Telescope Array", Opt. Eng., Vol. 27, No. 9, pp. 706-711, September 1988.

6. L. B. Mercer, "Adaptive Coherent Optical Receiver Array", Electron. Lett., Vol. 26, No. 18, August 1990.

7. W. M. Neubert et al., "Experimental Implementation of an Optical Multi-Aperture Antenna for Space Communications", Proc. SPIE, Vol. 1522, pp. 93-102, 1991.

8. K. H. Kudielka et al., "Experimental Verification of an Adaptive Optical Multi-Aperture Receive Antenna for Laser Space Communications", Proc. SPIE, Vol. 2123, paper 44, 1994.

9. W. M. Neubert et al., "Non-Mechanical Steering of Laser Beams by Multiple Aperture Antennas: Tolerance Analysis", Proc. SPIE, Vol. 1417, pp. 122-130, 1991.

10. W. M. Neubert et al., "Coherent Optical Self-Phasing Array Antenna for Space Communication Receivers", Proc. ECOC'93, Vol. 2, pp. 501-504, September 1993.

11. J. E. Pearson et al., "Coherent Optical Adaptive Techniques: Design and Performance of an 18-Element Visible Multidither COAT System", Appl. Opt., Vol. 15, No. 3, pp.611-621, March 1976.

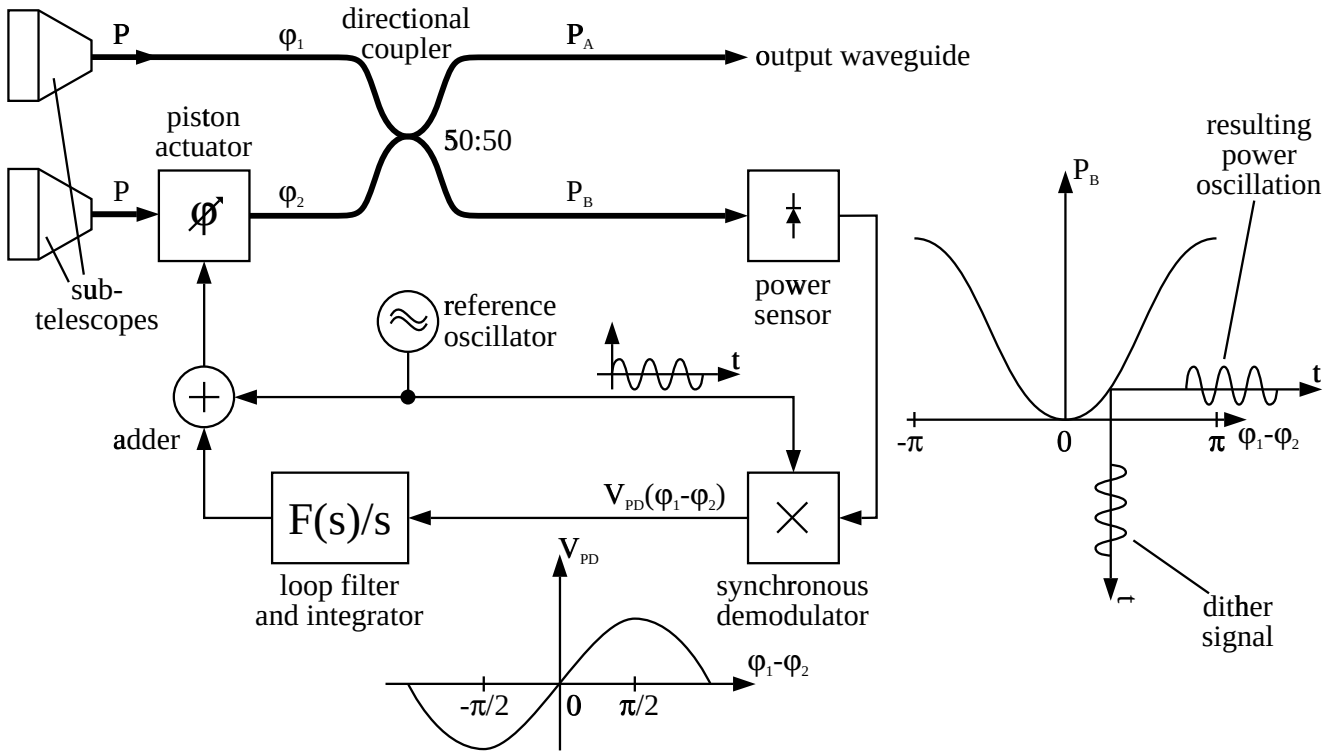

Fig. 1: Two-aperture RTA consisting of two subtelescopes, a piston actuator, a directional coupler, a power sensor, and a piston control unit. The total optical input power 2P is directed to the output waveguide.

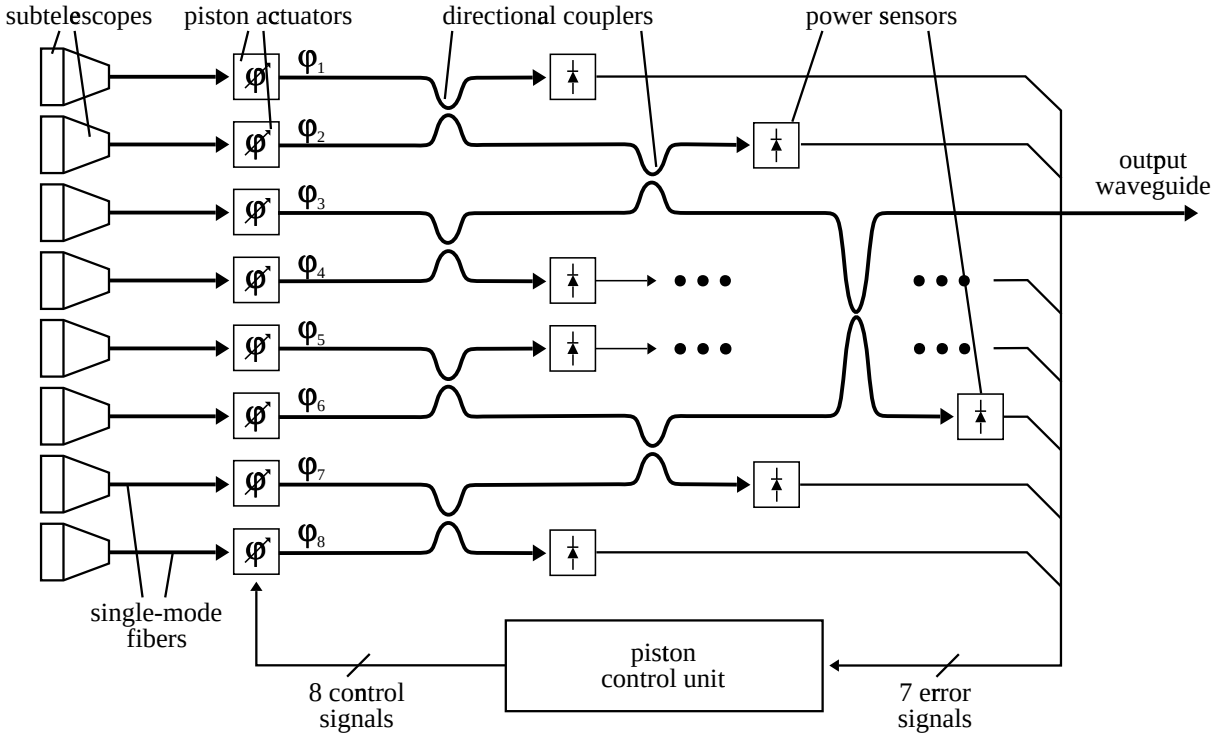

Fig. 2: Eight-aperture RTA (φ_k...optical subfield phases). The incident optical radiation is collected by subtelescopes and directed to a single output waveguide.

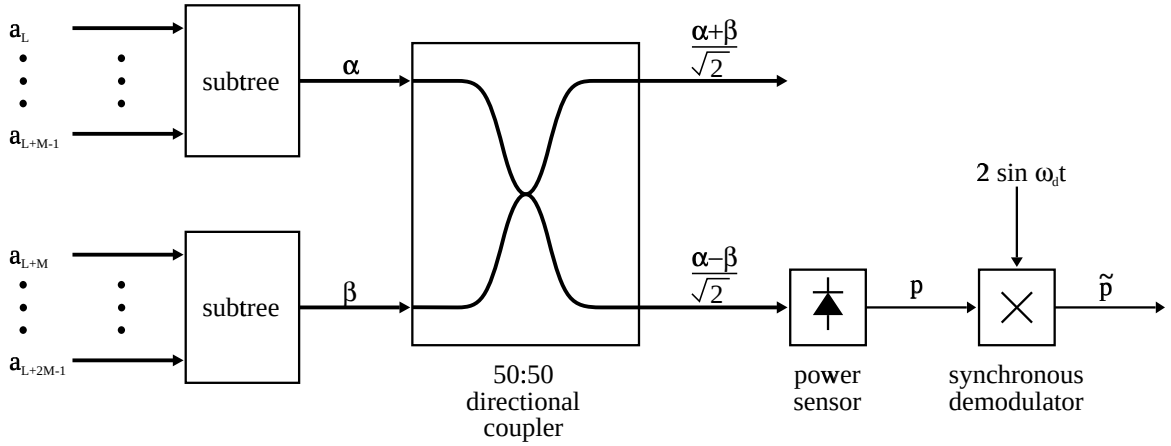

Fig. 3: Piston measurement within the directional coupler tree. Two subtrees feed a directional coupler. The ac signal resulting from piston dithering is detected by the optical power sensor and demodulated into the baseband (a_k,α,β...normalized optical fields, p...normalized optical power, ω_d...dither frequency).

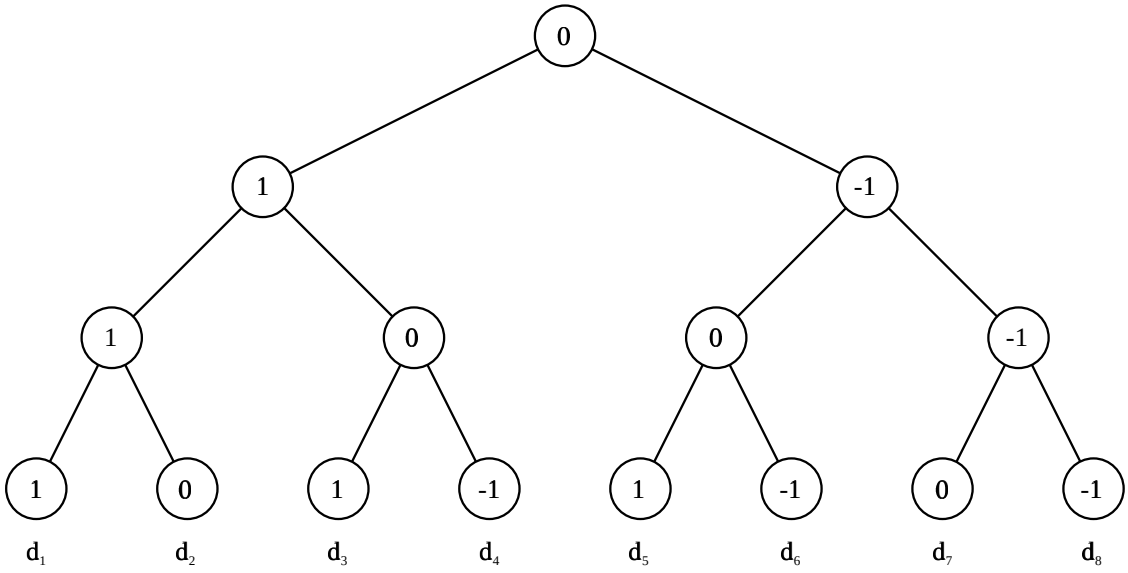

Fig. 4: Method to find a possible set of dither factors d_k for an eight-aperture RTA. The dither factors are the circled values at the bottom level.

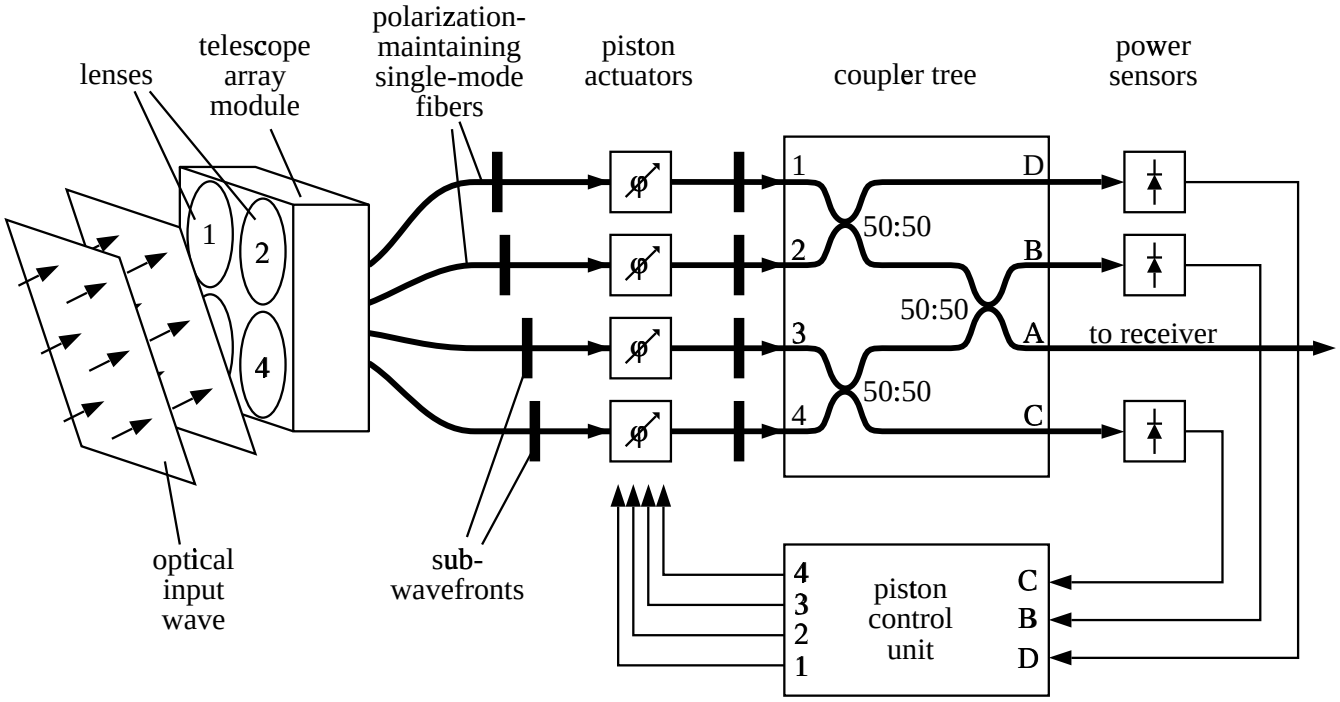

Fig. 5: Block diagram of the experimental four-aperture receive antenna. The incident optical radiation is collected by subtelescopes, coherently combined, and directed to a single output fiber.

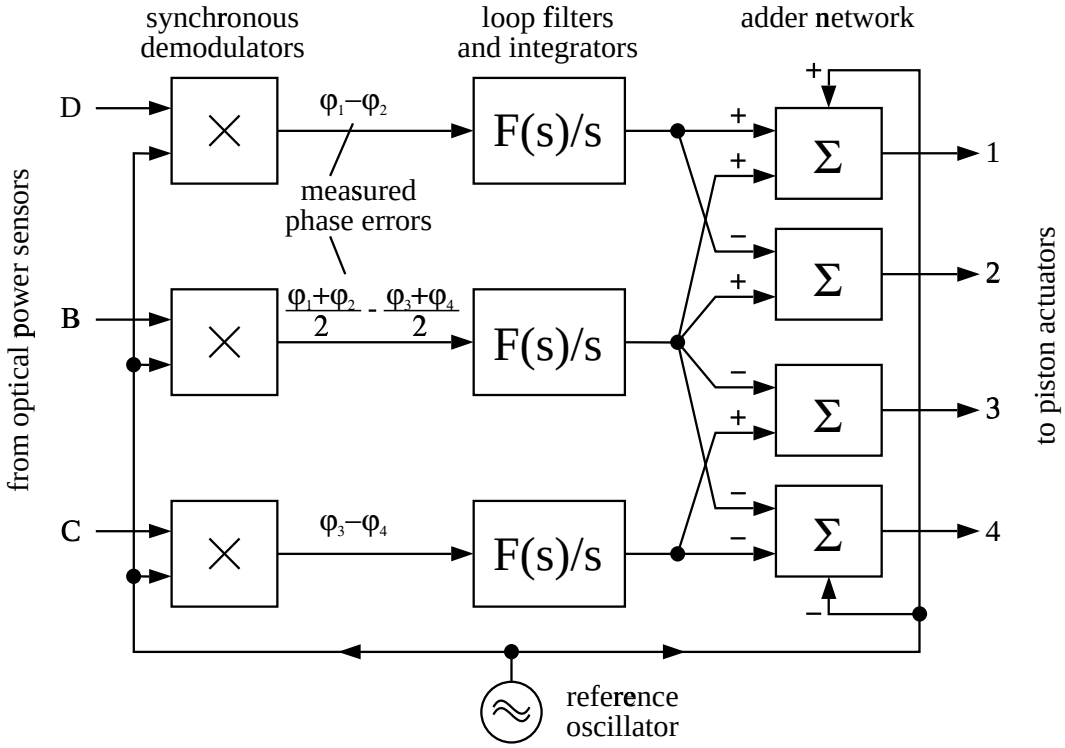

Fig. 6: Block diagram of the piston control unit.

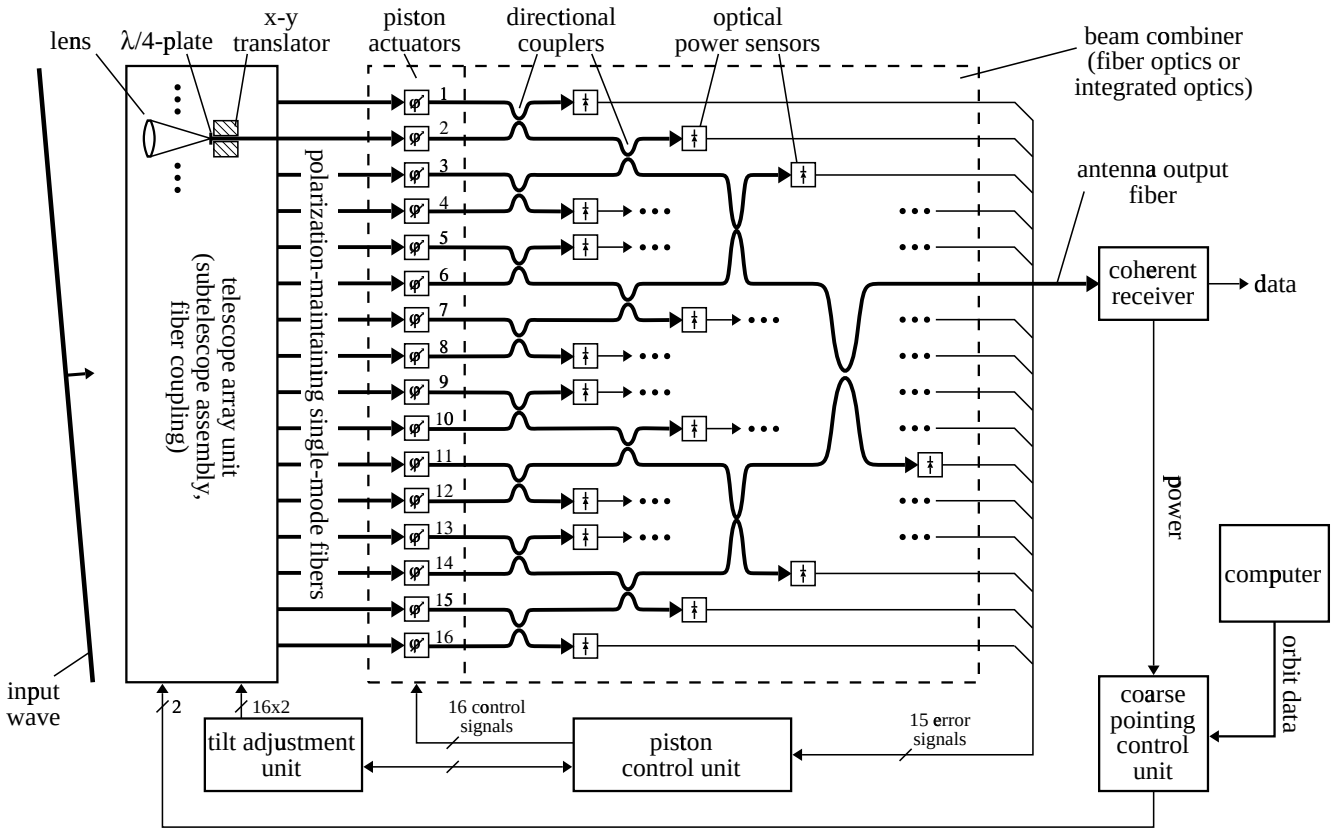

Fig. 7: Concept of a receive telescope array with 16 subtelescopes.

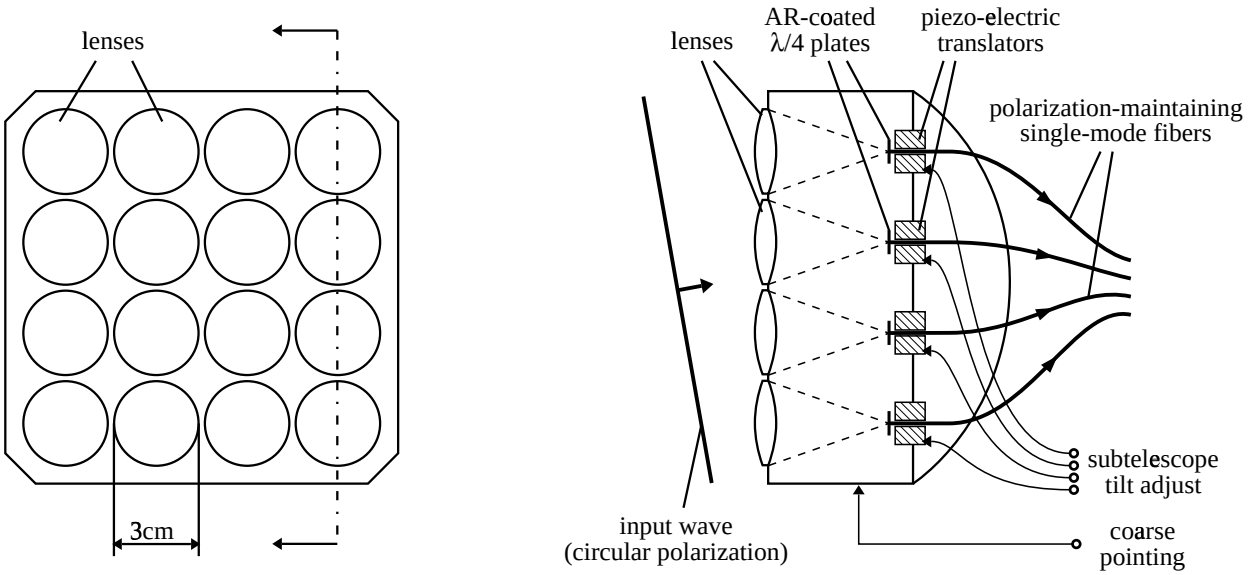

Fig. 8: Telescope array unit of the proposed RTA. Sixteen lenses couple the incident optical wave into polarization-maintaining single-mode fibers.